Oncogene (2005) 24, 5589–5605

www.nature.com/onc

Activation of the neuregulin-1/ErbB signaling pathway promotes the proliferation of neoplastic Schwann cells in human malignant peripheral nerve sheath tumors

Mark S Stonecypher[1,3], Stephanie J Byer[2], William E Grizzle[2] and Steven L Carroll*[,1,2]

[1]*Department of Cell Biology, The University of Alabama at Birmingham, Birmingham, AL 35294-0017, USA;* [2]*Department of Pathology, The University of Alabama at Birmingham, Birmingham, AL 35294-0017, USA;* [3]*The Medical Scientist Training Program, The University of Alabama at Birmingham, Birmingham, AL 35294-0017, USA*

Patients with neurofibromatosis type 1 develop aggressive Schwann cell neoplasms known as malignant peripheral nerve sheath tumors (MPNSTs). Although tumor suppressor gene mutations play an important role in MPNST pathogenesis, it is likely that dysregulated signaling by as yet unidentified growth factors also contributes to the formation of these sarcomas. To test the hypothesis that neuregulin-1 (NRG-1) growth factors promote mitogenesis in MPNSTs, we examined the expression and action of NRG-1 in human MPNSTs and neurofibromas, the benign precursor lesions from which MPNSTs arise. Multiple α and β transmembrane precursors from the class II and III NRG-1 subfamilies are present in both tumor types. Neoplastic Schwann cells within these neoplasms variably express the erbB kinases mediating NRG-1 responses (erbB2, erbB3 and/or erbB4). Human MPNST cell lines (Mash-1, YST-1, NMS-2 and NMS-2PC cells) similarly coexpress multiple NRG-1 isoforms and erbB receptors. These MPNST lines are NRG-1 responsive and demonstrate constitutive erbB phosphorylation. Treatment with PD168393 and PD158780, two structurally and mechanistically distinct erbB inhibitors, abolishes erbB phosphorylation and reduces DNA synthesis in these lines. These findings suggest that autocrine and/or paracrine NRG-1/erbB signaling promotes neoplastic Schwann cell proliferation and may be an important therapeutic target in neurofibromas and MPNSTs.
Oncogene (2005) **24,** 5589–5605. doi:10.1038/sj.onc.1208730; published online 9 May 2005

Keywords: ErbB receptors; neuregulin-1; neurofibromatosis; malignant peripheral nerve sheath tumor; neurofibroma

*Correspondence: SL Carroll, Division of Neuropathology, Department of Pathology, The University of Alabama at Birmingham, 1720 Seventh Avenue South, SC843, Birmingham, AL 35294-0017, USA; E-mail: carroll@path.uab.edu
Received 17 November 2004; revised 29 March 2005; accepted 29 March 2005; published online 9 May 2005

Introduction

Neurofibromatosis type 1 (NF1) is an autosomal dominant tumor predisposition syndrome that affects 1 in 3500 individuals (Gutmann *et al*., 1997; Parada, 2000; Gutmann, 2001). NF1 patients develop multiple types of neoplasms, including benign peripheral nerve sheath tumors known as neurofibromas that occur in skin (dermal neurofibromas), spinal and cranial nerve roots (intraneural or nodular neurofibromas) and large nerve plexuses (plexiform neurofibromas). Neurofibromas are infiltrating neoplasms composed of multiple cell types, with Schwann cells representing 40–80% of the tumor, and fibroblasts, perineurial cells, mast cells and vascular elements making up the remainder (Tucker and Friedman, 2002). Although dermal neurofibromas rarely undergo malignant transformation, plexiform and, less frequently, intraneural neurofibromas may progress and become malignant peripheral nerve sheath tumors (MPNSTs), a highly aggressive form of Schwann cell neoplasm (Ferner and O'Doherty, 2002). The prognosis for patients with MPNSTs is poor, with only 23% of these individuals alive 10 years after diagnosis (Ducatman *et al*., 1986; Woodruff *et al*., 2000). Beyond surgery, few therapeutic options are available for patients with MPNSTs (Ferner and Gutmann, 2002). Postsurgical irradiation of the tumor bed helps control local disease and delays tumor recurrence, but has no effect on overall survival (Ferner and O'Doherty, 2002). At present, no effective chemotherapeutic regimens are available for MPNSTs (Ferner and Gutmann, 2002). Because of these limitations, there is considerable interest in establishing the mechanisms responsible for MPNST tumorigenesis and using this information to develop new, more effective, therapies.

Mutations in tumor suppressor genes such as *NF1* (Legius *et al*., 1993; Metheny *et al*., 1995; Kluwe *et al*., 1999; Lakkis and Tennekoon, 2000; Parada, 2000; Rutkowski *et al*., 2000; Sherman *et al*., 2000; Wallace *et al*., 2000; Perry *et al*., 2001; Zhu and Parada, 2001; Ferner and O'Doherty, 2002; Tucker and Friedman, 2002), *p53* (Menon *et al*., 1990; Legius *et al*., 1994; Kourea *et al*., 1999a; Birindelli *et al*., 2001) and *INK4A* (also known as *CDKN2A*/*p16*) (Kourea *et al*., 1999b;

Nielsen *et al*., 1999) play an important role in the pathogenesis of neurofibromas and MPNSTs. However, it is likely that tumor suppressor mutations alone are not sufficient to induce peripheral nerve sheath tumor formation and that other abnormalities such as dysregulated growth factor signaling act cooperatively with these mutations to promote neurofibroma and MPNST tumorigenesis (Carroll and Stonecypher, 2004; Carroll and Stonecypher, 2005). We have hypothesized that inappropriate signaling by proteins in the neuregulin-1 (NRG-1) family of growth and differentiation factors contributes to the pathogenesis of peripheral nerve sheath tumors. NRG-1 proteins stimulate the proliferation, survival and migration of developing Schwann cells (Dong *et al*., 1995; Morrissey *et al*., 1995; Rahmatullah *et al*., 1998), and activating mutations of the NRG-1 receptor subunit erbB2 promote MPNST formation in rodents exposed to the mutagen *N*-ethyl-*N*-nitrosourea (EtNU) *in utero* (Bargmann *et al*., 1986; Hudziak *et al*., 1987; Bargmann and Weinberg, 1988; Weiner *et al*., 1989; Di Marco *et al*., 1990; Nikitin *et al*., 1991; Sherman *et al*., 1999). We have found that JS1 cells, a rat cell line derived from an EtNU-induced MPNST, lack this erbB2 mutation and express erbB2 in combination with the NRG-1 receptor subunit erbB3 and multiple NRG-1 isoforms. The NRG-1/erbB signaling pathway is constitutively activated in JS1 cells and the proliferation of this line is profoundly reduced by pharmacologic inhibition of erbB signaling (Frohnert *et al*., 2003a). We have also generated transgenic mice expressing the NRG-1 isoform glial growth factor-β3 (GGFβ3) in myelinating Schwann cells (P_0-GGFβ3 mice) (Huijbregts *et al*., 2003) and have found that these animals develop MPNST-like Schwann cell neoplasms with a latency of 6–12 months. GGFβ3 expression is maintained in these neoplasms and they markedly overexpress NRG-1 receptor subunits, suggesting that autocrine or paracrine NRG-1 signaling is essential for tumorigenesis in P_0-GGFβ3 mice. Considered together, these findings indicate that constitutive activation of the NRG-1/erbB signaling pathway promotes MPNST pathogenesis in rodents.

It is not yet known if the rodent models noted above are relevant to human neurofibroma and MPNST pathogenesis. To test the hypothesis that constitutive activation of the NRG-1/erbB signaling pathway promotes neoplastic Schwann cell proliferation in human peripheral nerve sheath tumors, we have examined human neurofibromas and MPNSTs to determine whether they express NRG-1 isoforms and the erbB kinases necessary for NRG-1 responsiveness and whether erbB signaling is essential for the proliferation of human MPNST cells.

Results

Neurofibromas and MPNSTs express multiple NRG-1 immunoreactive proteins

We prepared lysates from a series of these tumors (Table 1) and probed immunoblots of the lysates with a rabbit polyclonal antibody that recognizes an epitope within the EGF-like common domain present in all functional NRG-1 isoforms (a 'pan' NRG-1 antibody) (Carroll *et al*., 1997); a lysate of normal human sciatic nerve collected from an autopsied patient was included as a positive control. Multiple NRG-1 immunoreactive species ranging in size from 20 to 150 kDa were evident in all of the neurofibromas examined (Figure 1a). The masses of the most abundant larger (120 and 150 kDa) species detected in these neurofibromas are consistent with the masses of NRG-1 transmembrane precursors we have previously detected in nervous system tissues using this antibody (Carroll *et al*., 1997). Likewise, the smaller (20, 45 and 58 kDa) NRG-1 immunoreactive proteins migrate at the positions expected for the extracellular domains of proteolytically cleaved NRG-1 transmembrane precursors or directly secreted NRG-1

Table 1 Characteristics of nerve sheath tumors used for protein and RNA analyses

Case no.	*Diagnosis*	*Location*	*Age/race/gender*	*NF status*
1	Neurofibroma	Back	53/U/F	NF1
2	Neurofibroma	Retroperitoneum	45/W/M	NF1
3	Neurofibroma	Sciatic	45/W/M	NF1
4	Neurofibroma	Left buttock	17/B/M	NF1
5	Neurofibroma	Cervical	27/W/M	NF1
6	Neurofibroma	Cervical	38/B/M	NF1
7	Neurofibroma	Cervical	22/B/F	NF1
8	Neurofibroma	Left buttock	24/U/F	NF1
1	MPNST (epithelioid)	Lower Abdomen/groin	54/W/M	Unknown
2	MPNST	Right peroneal nerve	40/U/F	NF1
3	MPNST	Brain metastasis	62/W/F	NF1
4	MPNST	Right posterior thigh mass	46/W/M	NF1
5	MPNST	Retroperitoneal	20/B/M	NF1
6	MTT	Peritoneum	40/W/F	NF1
7	MPNST	Median nerve, right arm	16/B/M	NF1

Case numbers correspond to cases indicated in Figures 1–4

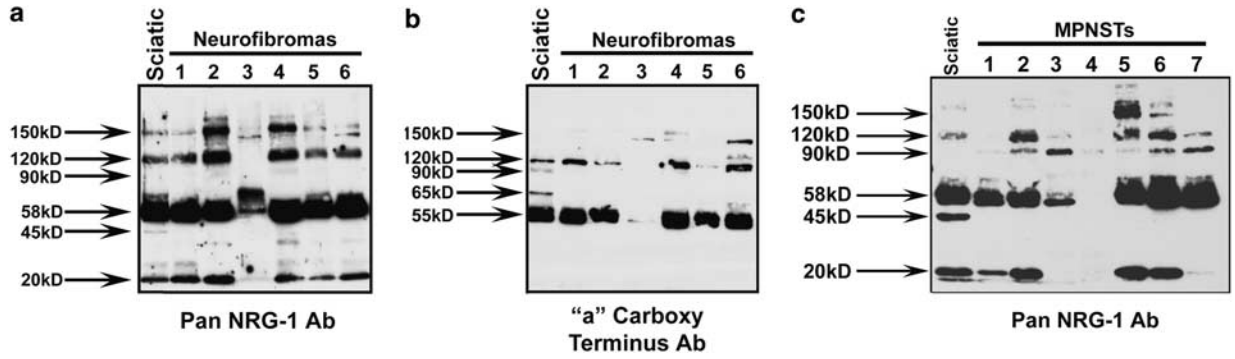

Figure 1 (**a**) Immunoblot of lysates of human sciatic nerve (Sciatic) and six human neurofibromas probed with a rabbit polyclonal antibody recognizing an epitope within the EGF-like common domain found in all NRG-1 isoforms. (**b**) Immunoblot of lysates of human sciatic nerve and human neurofibromas probed with a rabbit polyclonal antibody recognizing an epitope within the subset of NRG-1 transmembrane isoforms containing an 'a' variant carboxy terminus. (**c**) Immunoblot of lysates of human sciatic nerve (Sciatic) and seven human MPNSTs probed with a rabbit polyclonal antibody recognizing an epitope within the EGF-like common domain found in all NRG-1 isoforms. Arrows to the left of each panel indicate the major immunoreactive species and their molecular weights

isoforms (Ben-Baruch and Yarden, 1994; Carroll *et al*., 1997; Falls, 2003). Comparing the sizes of the NRG-1-like proteins detected in neurofibromas with those evident in normal sciatic nerve, a tissue type we have previously shown contains multiple NRG-1 isoforms (Carroll *et al*., 1997), we found that the NRG-1 immunoreactive species detected in neurofibromas comigrated with those evident in sciatic nerve. To further establish the identity of the proteins detected with the pan NRG-1 antibody, these same lysates were also probed with a second antibody that recognizes a subset of NRG-1 isoforms (transmembrane precursors with an 'a' variant carboxy-terminus). This antibody, like the pan NRG-1 antibody, recognized a 120 kDa species in the majority of the neurofibromas, with a 150 kDa protein also evident in some tumors (Figure 1b). The anti-'a' carboxy-terminus antibody also labeled a prominent 55 kDa protein in sciatic nerve and neurofibromas and a 65 kDa polypeptide in sciatic nerve. These latter polypeptides are too small to be full-length NRG-1 transmembrane precursor proteins and likely represent recently described NRG-1 proteolytic cleavage products thought to mediate 'back-signaling' into the interior of NRG-1-expressing cells (Bao *et al*., 2003). We conclude that neurofibromas express multiple NRG-1 immunoreactive proteins, some of which are NRG-1 transmembrane precursors.

To ascertain whether MPNSTs also express NRG-1 proteins, lysates were prepared from seven surgically resected MPNSTs (Table 1), immunoblotted and probed with the pan NRG-1 antibody. We found that these neoplasms, like neurofibromas, express multiple NRG-1 isoforms (Figure 1c) with masses similar to those of the NRG-1 immunoreactive species detected in neurofibromas. The only difference was that the masses of the higher molecular weight NRG-1 proteins present in MPNSTs were more variable than those evident in neurofibromas, with a 90 kDa protein (which was also evident in neurofibromas with long exposures (data not shown)) being much more prominent in MPNSTs. It was thus apparent that MPNSTs, like neurofibromas, express multiple NRG-1 immunoreactive proteins.

Neurofibromas and MPNSTs express a complex mixture of α and β transmembrane precursors from the class II and III NRG-1 subfamilies

The *NRG1* locus, using a combination of alternative splicing and transcription from multiple promoters, produces at least 15 NRG-1 isoforms with distinct structural and functional characteristics (Falls, 2003). To determine whether the variably sized proteins detected by the pan NRG-1 antibody in human neurofibromas and MPNSTs represent distinct NRG-1 splice variants, we examined the structure of the NRG-1 transcripts expressed in these neoplasms. NRG-1 activation of erbB kinases is mediated by the EGF-like domain, which is composed of an amino-terminal invariant (common) domain coupled to α or β variant domains (Figure 2a, left panel); NRG-1 α and β isoforms are functionally distinct, differing both in their affinities for NRG-1 receptors and their ability to elicit at least some biologic responses (Falls, 2003). The EGF-like domain is followed by a structurally variable juxtamembrane domain, which determines whether the protein is synthesized as a directly secreted form or as a transmembrane precursor requiring proteolytic cleavage for release. As all functional NRG-1 isoforms must contain a receptor binding domain, we used PCR to amplify NRG-1 sequences encoding a region encompassing the EGF-like common, EGF-like variant (α or β), juxtamembrane (1, 2 or 4 variant) and transmembrane domains from six neurofibromas and six MPNSTs. These sequences were detectable in all of the neurofibromas and MPNSTs tested (data not shown). To further examine the protein structures predicted by these NRG-1 sequences, the PCR products amplified from two neurofibromas and two MPNSTs were cloned and multiple subclones sequenced. We found that the NRG-1 transmembrane precursors expressed in these neoplasms were structurally diverse and included NRG-1 β1, β2 and α2 variants (Figure 2a). In contrast, sequences encoding the EGF-like domain of NRG-1 secreted isoforms (isoforms with a '3' variant juxtamembrane domain) could not be amplified from

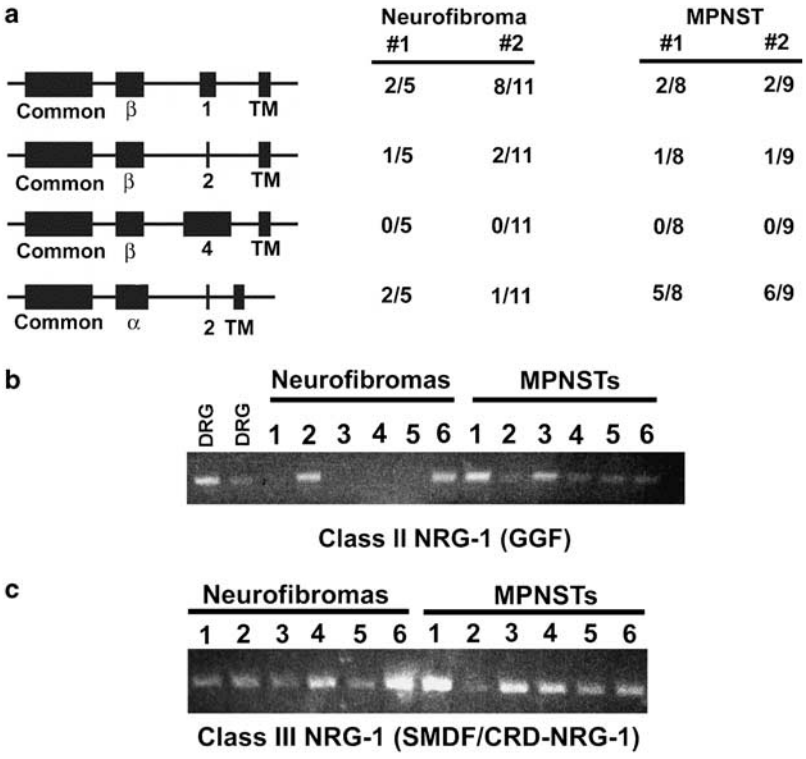

Figure 2 Neurofibromas and MPNSTs express mRNAs encoding a complex mixture of NRG-1 transmembrane precursors including α and β isoforms from the class II and III NRG-1 subfamilies. (**a**) Structures of the EGF-like and adjacent domains hypothetically possible in NRG-1 isoforms expressed in MPNSTs. Domain designations: Common, the NRG-1 EGF-like common domain; α or β, EGF-like variant domains; 1, 2 or 4, juxtamembrane domains; TM, transmembrane domain. Ratios to the right of each diagram indicate the number of times a structural variant was isolated divided by the total number of clones sequenced. (**b**) PCR analysis of class II NRG-1 (GGF) mRNA expression in human neurofibromas and MPNSTs. DRG cDNAs from two autopsied patients were included as positive controls. (**c**) PCR analysis of class III NRG-1 (SMDF/cysteine-rich domain NRG-1) mRNA expression in human neurofibromas and MPNSTs. Images in panels b and c are photographs of ethidium bromide-stained gels

neurofibroma and MPNST cDNAs, although these primers did produce a PCR product of the appropriate size from control cDNAs (data not shown).

Three NRG-1 subfamilies (class I, II and III NRG-1 isoforms) are known, each defined by a unique amino-terminal sequence that confers distinctive biologic characteristics on the protein (Falls, 2003). To establish which NRG-1 subfamilies are expressed in human neurofibromas and MPNSTs, PCR was performed with cDNAs derived from six neurofibromas and six MPNSTs using primers specific for sequences encoding each of the three distinct NRG-1 amino-terminal domains. Class II (GGF) NRG-1 transcripts were detected in two of six neurofibromas and in all six MPNSTs (Figure 2b). RNA encoding class III (sensory and motor neuron-derived factor (SMDF)/cysteine-rich domain) NRG-1 isoforms was present in all neurofibromas and MPNSTs tested (Figure 2c). In contrast, although readily amplified from control specimens, class I (neu differentiation factor (NDF)) NRG-1 transcripts were not detected in any of the neurofibromas and MPNSTs examined (data not shown). We conclude that human neurofibromas and MPNSTs express a complex mixture of α and β transmembrane precursors from the class II and III NRG-1 subfamilies.

Human neurofibromas and MPNSTs express the erbB membrane tyrosine kinases necessary for NRG-1 responsiveness

NRG-1 binds directly to the erbB3 (HER3) or erbB4 (HER4) membrane tyrosine kinases, an event that promotes homo- or heterodimerization with other erbB family members (Yarden and Sliwkowski, 2001), with erbB2 (c-*neu*, HER2) being the preferred partner for both NRG-1 receptors (Tzahar *et al*., 1996; Graus-Porta *et al*., 1997). The erbB kinases mediating NRG-1 responses are also capable of heterodimerizing to and thus 'crosstalking' with the EGF receptor (EGFR, erbB1), a molecule whose expression is increased (DeClue *et al*., 2000) in many peripheral nerve sheath tumors (Perry *et al*., 2002). To determine whether NRG-1 receptors are expressed in peripheral nerve sheath tumors and to examine the relationship between the expression of receptors for NRG-1 and EGF, we immunoblotted lysates of surgically resected neurofibromas and MPNSTs and probed them with antibodies recognizing EGFR, erbB2, erbB3 or erbB4. In human neurofibromas, EGFR was detected in five of six tumors examined (Figure 3) and was expressed at very high levels in two neoplasms and at moderate levels in several

others. ErbB2 (c-*neu*) was evident in two neurofibromas (Figure 3), while erbB3 was present in all six neurofibromas, with strikingly high levels of expression in four tumors (Figure 3). A protein of the expected 185 kDa mass was also detected in two neurofibromas with an anti-erbB4 antibody (Figure 3). PCR analyses of erbB expression in these neoplasms confirmed the expression patterns observed by immunoblot analyses and indicated that erbB2 and erbB3 mRNA was detectable in all six neurofibromas (data not shown), suggesting that some neoplasms expressed relatively low levels of these kinases or that erbB2 and erbB3 expression is confined to a subpopulation of cells within these tumors.

In human MPNSTs, EGFR was present in six of the seven tumors studied (Figure 4); this kinase was expressed at very high levels in three neoplasms. ErbB2 was detected in five tumors (Figure 4), with erbB2 levels in three of the neoplasms being comparable to those in JS1 MPNST cells, a line we have shown overexpresses both erbB2 and erbB3 relative to non-neoplastic adult Schwann cells (Frohnert *et al*., 2003a). ErbB3 was readily detected in six of seven human MPNSTs, with strikingly high levels of expression observed in four tumors (Figure 4). The anti-erbB4 antibody detected a protein of the expected 185 kDa mass in two MPNSTs (Figure 4), with a slightly smaller erbB4 immunoreactive protein evident in a third tumor.

To establish whether erbB kinases and NRG-1 within peripheral nerve sheath tumors were predominantly associated with tumor cells or non-neoplastic elements such as the abundant vasculature characteristic of these neoplasms, sections of a second series of neurofibromas and MPNSTs (Table 2) were immunostained with the 'pan' NRG-1 antibody or antibodies recognizing EGFR, erbB2, erbB3 or erbB4. EGFR immunoreactivity was detected in a subset of neurofibromas (three of seven tumors; Figure 5 and Table 2) and MPNSTs (three of five tumors; Figure 5 and Table 2), while erbB2 labeling was uniformly present in neurofibromas and MPNSTS (Figure 5 and Table 2). Expression of the direct NRG-1 receptor, erbB3, was detected in five out of seven neurofibromas and in three out of five MPNSTs

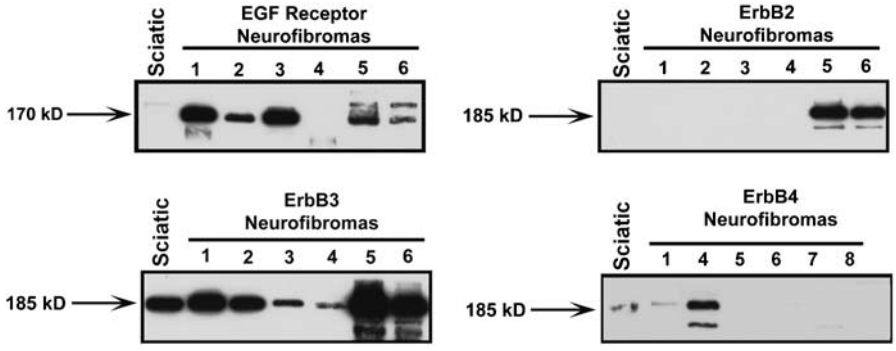

Figure 3 EGFR, erbB2, erbB3 and erbB4 protein expression in human neurofibromas. Arrows to the left of each panel indicate the expected position of each erbB kinase; in our experience, minor variability in the size of erbB kinases (potentially resulting from differences in post-translational modification) is frequently encountered in tumors overexpressing an erbB kinase. Lysates of human sciatic nerve and, in some blots JS1 MPNST cells, were included as controls. Numbers above each lane indicate the case number corresponding to the clinical information presented in Table 1. Longer exposures of the erbB2 blot showed that erbB2 expression was also present in sciatic nerve (data not shown; see also Figure 4). The quantity of lysate available from tumors 2 and 3 was insufficient for examination of erbB4 expression, so two additional tumors (7 and 8) were obtained and probed for this receptor

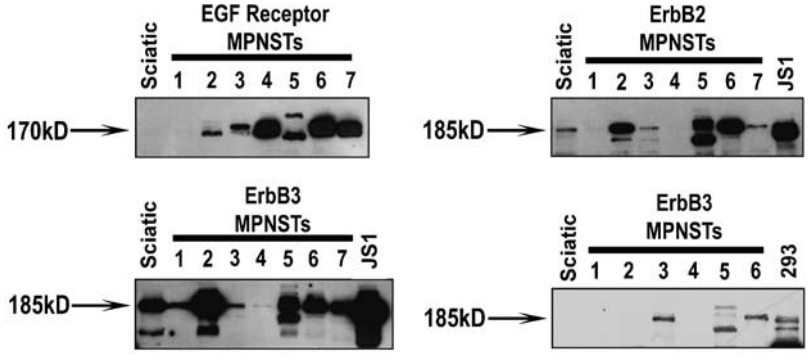

Figure 4 EGFR, erbB2, erbB3 and erbB4 protein expression in human MPNSTs. Arrows to the left of each panel indicate the expected position of each erbB kinase. Lysates of human sciatic nerve and, in some blots JS1 MPNST cells or 293 cells, were included as positive controls. Numbers above each lane indicate the case number corresponding to the clinical information presented in Table 1. Longer exposures of the erbB4 blot (not shown) showed low levels of erbB4 expression in sciatic nerve as were observed in Figure 3

Table 2 NRG-1 and ErbB immunoreactivity in human neurofibromas and MPNSTs

Case no.	*Diagnosis*	*Location*	*Age/race/gender*	*NF status*	*ErbB-1*	*ErbB-2*	*ErbB-3*	*ErbB-4*	*NRG-1*
9	Neurofibroma	C1–C2 nerve root	38M	Unknown	–	+	–	–	–
10	Neurofibroma	C1–C2 nerve root	63M	Unknown	–	+	–	–	+
11	Neurofibroma	Cervical nerve root	21F	NF1	–	+	+	–	+
12	Neurofibroma	Gastric plexus	43/W/F	NF1	+	+	+	+	+
13	Neurofibroma	Left leg	43/W/F	NF1	+	+	+	+	+
14	Neurofibroma	Right neck	42/B/M	NF1	+	+	+	+	+
15	Neurofibroma	C1–C2 nerve root	74M	Unknown	–	+	+	+	–
8	MPNST	Left buttock	33/B/F	Unknown	+	+	+	+	+
9	MPNST	Left buttock	33/B/F	Unknown	+	+	+	+	+
10	MPNST	Left thigh	31/B/F	NF1	+	+	+	–	+
11	MPNST	Brain metastasis	62/W/F	NF1	–	+	+	+	+
12	MPNST	Right thigh	14/B/M	NF1	–	+	–	–	+

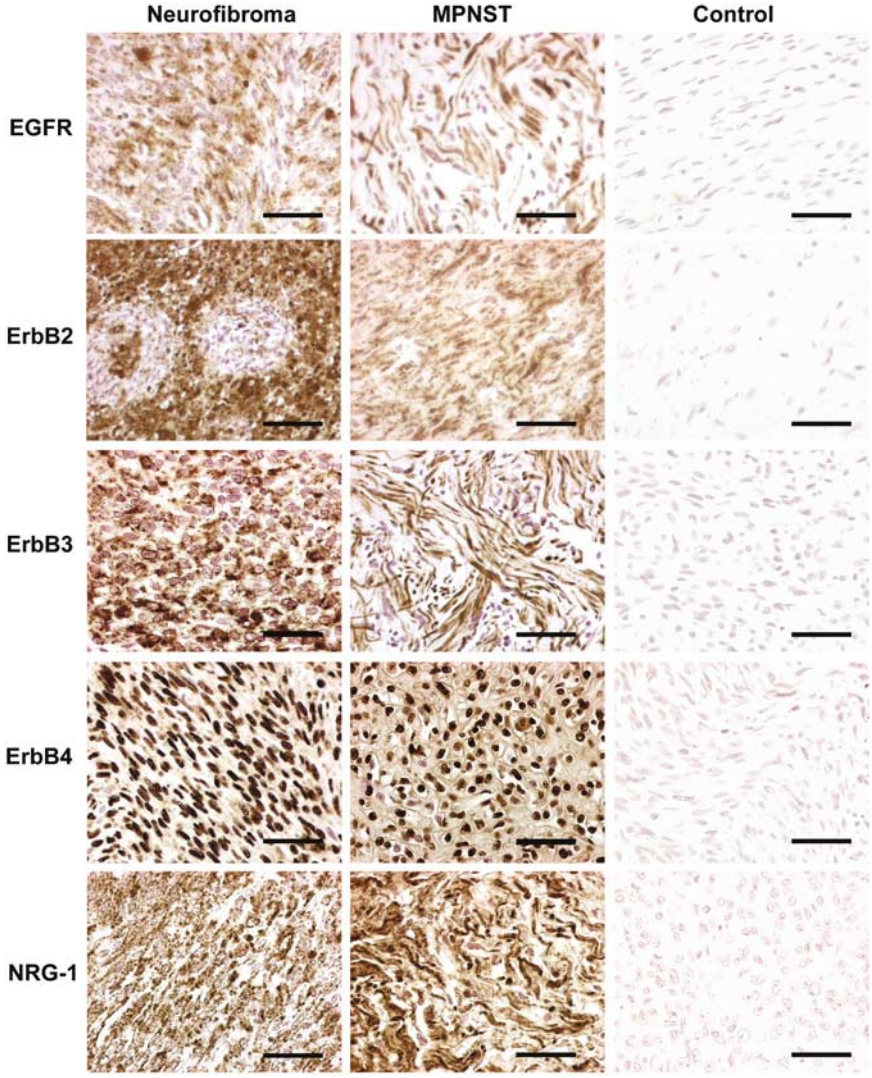

Figure 5 ErbB and NRG-1 immunoreactivity in human neurofibromas and MPNSTs. Shown are representative photomicrographs of neurofibromas (left column) and MPNSTs (middle column) immunostained for EGFR, erbB2, erbB3, erbB4 or the NRG-1 EGF-like common domain (indicated to the left of each row). The right column demonstrates the staining evident in control sections (either immunostains in which the primary antibody was replaced with nonimmune immunoglobulin (EGFR and erbB3) or immunostains in which the primary antibody was preincubated with the immunizing peptide (erbB2, erbB4 and NRG-1). These sections have been lightly counterstained with hematoxylin. Scale bar, 50 μm

(Figure 5 and Table 2). ErbB4 immunoreactivity was less common, being found in four neurofibromas and one MPNST. NRG-1 and each of the erbB receptors were predominantly associated with cells within the tumor mass, demonstrating distinct cellular distributions in neurofibroma and MPNST cells. EGFR, erbB2 and erbB3 immunoreactivity was evident as cytoplasmic and membranous staining. In contrast, erbB4 immunoreactivity was predominantly associated with nuclei and surface membranes; the presence of nuclear immunoreactivity is consistent with previous studies demonstrating that activated erbB4 is proteolytically cleaved and its carboxy terminus translocated to the nucleus (Carpenter, 2003). NRG-1 immunoreactivity was also associated with the cytoplasm and surface membranes of tumor cells and thus has a distribution similar to that of EGFR, erbB2 and erbB3. These results, considered together with our PCR and immunoblot analyses, indicate that the majority of human MPNSTs express NRG-1 in combination with the erbB kinases necessary for NRG-1 responsiveness.

MPNST cell lines express multiple NRG-1 isoforms and the erbB membrane kinases mediating NRG-1 responses

The coexpression of multiple NRG-1 isoforms and their receptors in neurofibromas and MPNSTs raised the question whether these molecules are expressed by the same cells and thus capable of stimulating proliferation or other effects by autocrine and/or paracrine signaling. To test this hypothesis, we assembled a panel of human MPNST cell lines derived from NF1-associated (Mash-1 (Endo *et al*., 2002), NMS-2 (Imaizumi *et al*., 1998) and NMS-2PC (Imaizumi *et al*., 1998) cell lines) or sporadically arising (YST-1 cells; Nagashima *et al*., 1990) MPNSTs. Prior to examining NRG-1 and erbB expression in these lines, we verified their lineage by immunostaining cells grown in chamber slides or embedded in tissue arrays with a panel of antibodies recognizing Schwann cell, neuronal or muscle markers. Mash-1 (Figure 6a), YST-1 (Figure 6b), NMS-2 (Figure 6c) and NMS-2PC (Figure 6d) cells all demonstrated cytoplasmic and nuclear immunoreactivity for the Schwann cell marker S100β, which was abolished when the primary antibody was replaced with nonimmune IgG (Figure 6e). All four lines also showed cytoplasmic immunoreactivity for collagen type IV (data not shown), a basal lamina protein elaborated by Schwann cells. Immunoreactivity for glial fibrillary acidic protein (GFAP), the neuronal marker neuron-specific enolase (NSE) and the muscle marker desmin was not evident in any of these lines. However, a subpopulation of cells within three of the MPNST lines stained for smooth muscle actin (Figure 6f), suggesting that these lines, like a subset of MPNSTs (e.g. malignant Triton tumors), have a potential for divergent differentiation. To further test this hypothesis, we examined the expression of mRNAs encoding 18 Schwann cell, neuronal and muscle markers in all four lines using RT-PCR (Figure 6g). In addition to the markers noted above, we found that these lines uniformly express transcripts encoding the Schwann cell markers myelin protein zero (P_0), $p75^{LNTR}$, Sox10 and Krox 20, with several lines additionally expressing myelin basic protein, peripheral myelin protein-22 (PMP22), Pax3 and GAP43. mRNAs encoding the light neurofilament subunit were also present in all four lines, with transcripts for a second neuronal intermediate filament, peripherin, weakly detectable in YST-1 and NMS-2 cells. The muscle marker SM22α (transgelin) was additionally expressed by all four MPNST cell lines; other muscle markers were detectable only with difficulty in some lines (calponin-1, desmin) or completely undetectable (MyoD1). We conclude that Mash-1, YST-1, NMS-2 and NMS-2PC cells express multiple Schwann cell markers and variably express neuronal and muscle markers, as expected for neoplastic elements derived from MPNSTs. Of note, the pattern of marker expression observed in these four human MPNST cell lines is similar to that found in cell lines derived from the MPNST-like tumors that develop in *Nf1*+/−:*p53* +/− mice (Vogel *et al*., 1999).

Probing lysates of the human MPNST cell lines with the 'pan' NRG-1 antibody, we found that multiple NRG-1 immunoreactive proteins were present in all four lines (Figure 7a). The major NRG-1 like proteins evident in these lines had masses of 45, 58, 120 and 150 kDa and thus comigrated with several of the NRG-1 species detected in surgically resected human neurofibromas and MPNSTs. Probing these same lysates with the antibody recognizing the subset of NRG-1 transmembrane precursors with an 'a' carboxy-terminal domain, we found that this antibody recognized proteins migrating at the same position as the two larger (120 and 150 kDa) NRG-1 proteins detected by the pan NRG-1 antibody (Figure 7b). As in tumor tissue and sciatic nerve, this antibody also labeled a 55 kDa protein in all four lines and a 65 kDa polypeptide present in YST-1 cells; the sizes of these immunoreactive species are consistent with those of intracellular domain fragments released from mature NRG-1 transmembrane precursors by proteolytic cleavage (Bao *et al*., 2003). Preincubation of the pan NRG-1 and 'a' carboxy-terminus antibodies with their immunizing peptide abolished or markedly diminished the NRG-1 immunoreactivity detected in these MPNST cell line lysates (Figure 7a and b), while preincubation with an unrelated antigen had no effect on the detected signals (data not shown).

The presence of variably sized NRG-1 immunoreactive proteins in the human MPNST lines suggested that these cells, like neurofibromas and MPNSTs *in vivo*, express multiple NRG-1 isoforms. To test this hypothesis, we examined the structure of the NRG-1 mRNAs expressed in each MPNST cell line. Using primers that amplify sequences encoding the EGF-like common, EGF-like variant, juxtamembrane and transmembrane domains, we detected NRG-1 transmembrane precursor transcripts in all four MPNST cell lines (Figure 7c, top panels). Expression of mRNAs encoding NRG-1 secreted isoforms was more limited, being evident only in YST-1 cells (Figure 7c, bottom panels). PCR

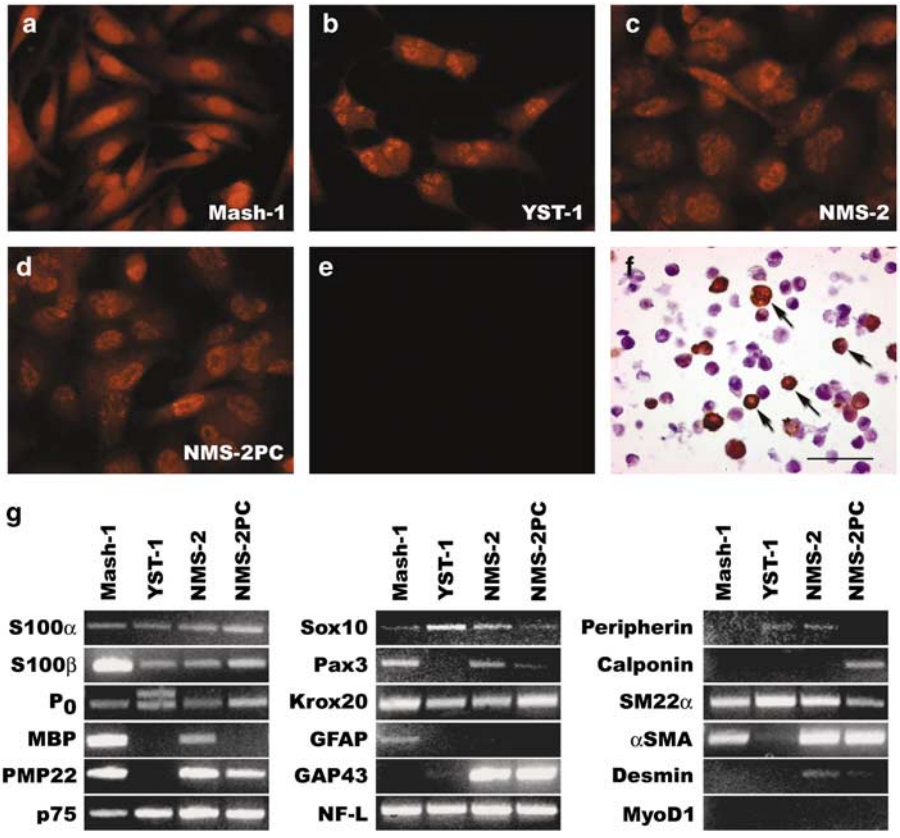

Figure 6 Human MPNST cell lines express multiple Schwann cell markers in combination with some neuronal and muscle markers. Shown are immunostains for the Schwann cell marker S100β in Mash-1 (**a**), YST-1 (**b**), NMS-2 (**c**) and NMS-2PC (**d**) cells. This immunoreactivity was not evident when the primary antibody was replaced with nonimmune IgG (**e**, representative photo of Mash-1 cells stained with nonimmune IgG). Tissue array section of NMS-2PC cells demonstrating immunoreactivity for smooth muscle actin in a subpopulation of these cells (**f**, arrows). Scale bar, 50 μm. (**g**), RT–PCR analyses of the expression of mRNAs encoding Schwann cell, neuronal and muscle markers in human MPNST cell lines. The identity of the tested cell lines is indicated above each lane, with markers indicated to the left of each panel. P_0, myelin protein zero; MBP, myelin basic protein; PMP22, peripheral myelin protein-22; p75, the p75 low-affinity neurotrophin receptor; GFAP, glial fibrillary acidic protein; NF-L, light neurofilament subunit; αSMA, α-smooth muscle actin

performed with primers hybridizing to sequences encoding the amino-terminal domain of class II (GGF) NRG-1 isoforms demonstrated that the NRG-1 transcripts detected in all four MPNST cell lines included members of this NRG-1 subfamily (Figure 7d, top panels), with class III (SMDF) NRG-1 mRNAs also present in NMS-2, NMS-2PC and YST-1 cells (Figure 7d, bottom panel). In contrast, class I (NDF) NRG-1 sequences were detectable only in YST-1 cells (data not shown). We conclude that NMS-2, NMS-2PC and YST-1 MPNST cells, like MPNSTs *in vivo*, express predominantly class II and III NRG-1 transmembrane precursor proteins. The diversity of NRG-1 isoforms expressed in Mash-1 cells is more restricted, consisting solely of class II NRG-1 transmembrane isoforms.

To establish whether each of the four MPNST cell lines expressed the erbB receptors necessary for NRG-1 responsiveness, we probed lysates of these cells with antibodies recognizing EGFR, erbB2, erbB3 or erbB4. We found that all four of these MPNST cell lines express a combination of erbB receptors that renders them potentially NRG-1 responsive (Figure 8a). Two lines (Mash-1 and NMS-2PC) express erbB2 together with erbB3, a combination of NRG-1 receptor subunits identical to that in non-neoplastic Schwann cells (Carroll *et al*., 1997), while a third (NMS-2 cells) expresses erbB2, erbB3 and erbB4. Although YST-1 cells did not contain detectable levels of erbB2, these cells coexpress erbB3 and erbB4; erbB4 is capable of heterodimerization with erbB3 or homodimerization with itself to form a functional NRG-1 receptor (Carpenter, 2003). Two MPNST cell lines (NMS-2 and NMS-2PC cells) also expressed EGFR, indicating that erbB signaling in these lines is potentially enhanced by coactivation of EGFR. EGFR was undetectable in lysates of Mash-1 and YST-1 cells.

In at least some cell types, erbB4 undergoes proteolytic cleavage and fragments from its carboxy terminus are transported to the nucleus, where they are thought to participate in as yet undefined signaling events (Carpenter, 2003). Probing immunoblots of NMS-2 and YST-1 lysates with an antibody recognizing the

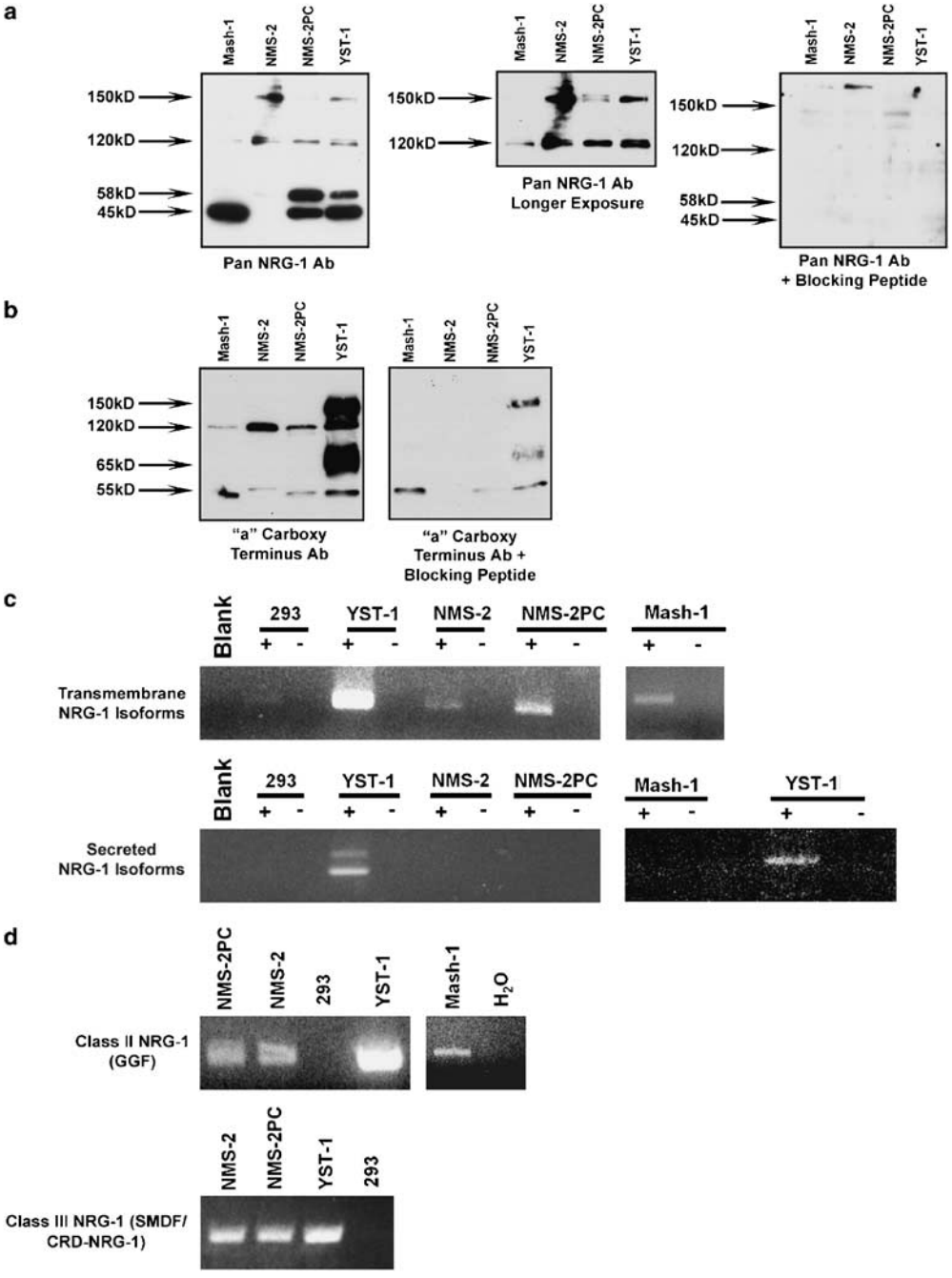

Figure 7 Human MPNST cell lines express multiple class II and III NRG-1 isoforms. (**a**), Lysates of human MPNST cell lines (indicated above each lane) probed with an antibody recognizing an epitope in the EGF-like common domain found in all NRG-1 isoforms (left panel). A longer exposure (middle panel) is included to better demonstrate the higher molecular weight NRG-1 proteins in each cell line. Preincubation with the immunizing peptide abolished labeling of these proteins (right panel). Arrows to the left of these three panels indicate the position and molecular weight of each protein. (**b**) A second antibody recognizing an epitope at the carboxy terminus of a major subset of NRG-1 isoforms (transmembrane precursors with an 'a' carboxy terminus) labels proteins with molecular weights similar to some detected with the pan NRG-1 antibody (left panel) as well as potential cleavage products (55 and 65 kDa species). Preincubation with the immunizing peptide abolished or markedly reduced labeling with this antibody (right panel). (**c**) PCR analyses of the expression of transmembrane and secreted NRG-1 isoforms in human MPNST cell lines. The identity of the cell lines is indicated above each lane; reverse-transcribed RNAs and reverse transcription reactions performed identically except for the addition of reverse transcriptase are indicated as + and −, respectively. Blank is a PCR reaction performed with distilled water substituted for cDNA. YST-1 cDNA was included in the second set of PCR reactions for secreted NRG-1 isoforms (right panel) as a positive control. (**d**) PCR detection of sequences encoding class II (upper panels) and III (lower panel) NRG-1 isoforms. A cDNA produced by reverse transcription of 293 cells (293) and a water blank (H_2O) were included as negative controls

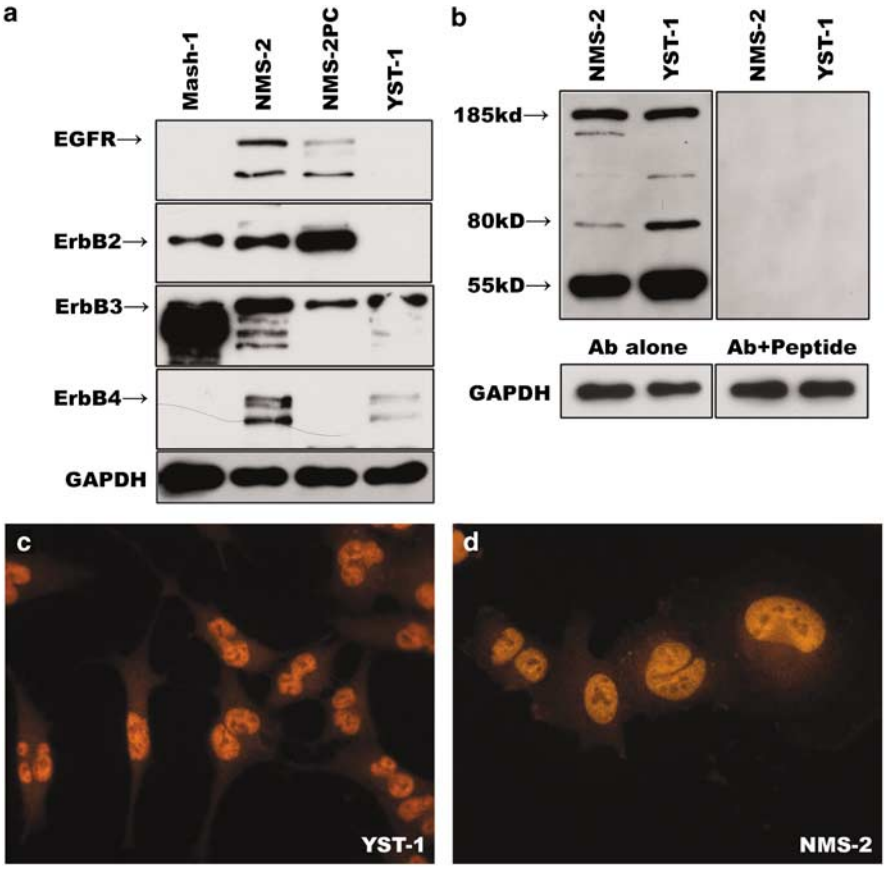

Figure 8 Human MPNST cell lines express varying combinations of the erbB kinases mediating NRG-1 responsiveness. (**a**) Immunoblot analyses of erbB expression in four human MPNST cell lines. The identity of the cell lines is indicated above each lane, with the specific full-length erbB receptor-(a 170 kDa protein for the EGFR; 185 kDa species for the other three erbB kinases) labeled by each antibody indicated to the left of the blots. GAPDH loading controls are shown below the erbB immunoblots. (**b**) Immunoblot analyses of the erbB4 immunoreactive species detectable in NMS-2 and YST-1 cells. Left panel, blots probed with anti-erbB4 antibody alone detect the 185 kDa full-length protein as well as some smaller species (indicated by arrows to the left of the panel). Right panel, preincubating the primary antibody with the immunizing peptide blocks the labeling of these species. GAPDH loading controls are indicated below each panel. (**c**, **d**), YST-1 and NMS-2 cells immunostained with the erbB4 antibody demonstrate prominent nuclear labeling in combination with cytoplasmic and/or membranous labeling

erbB4 carboxy terminus, we found that this antibody recognized both the full-length 185 kDa species and several smaller proteins (Figure 8b). These smaller polypeptides included a fragment similar in mass to a previously described erbB4 cleavage product (80 kDa; Carpenter, 2003) and a prominent 55 kDa species (Figure 8b, left panel). Preincubation with the immunizing peptide abolished labeling of both the full-length erbB4 protein and the smaller proteins (Figure 8b, right panel). Consistent with the hypothesis that erbB4 is proteolytically cleaved in MPNST cells and its carboxy terminus transported to the nucleus, prominent erbB4 immunoreactivity was found in the nuclei of YST-1 (Figure 8c) and NMS-2 (Figure 8d) cells, with lighter staining also evident in association with the cytoplasm and/or cellular membranes. As shown above, this pattern of erbB4 immunoreactivity is similar to that seen in neurofibromas and MPNSTs *in vivo* (see Figure 5).

Constitutive activation of erbB receptors promotes DNA synthesis in human MPNST cell lines

To determine whether human MPNST cells are responsive to NRG-1, Mash-1 cells, which express erbB2 and erbB3 in the absence of EGFR expression, were stimulated for 15 min with vehicle or NRG-1β (1, 10 or 50 nM). The direct NRG-1 receptor erbB3 was then immunoprecipitated from lysates of these cells, immunoblotted and probed with an antibody recognizing phosphotyrosine. Phosphorylated erbB3 was detected in these experiments as a band of the expected 185 kDa mass that increased in intensity with increasing concentrations of NRG-1β (Figure 9a). Pretreating cells with PD168393, a 6-acrylamido-4-anilinoquinazoline compound that irreversibly inhibits erbB receptors by forming a covalent bond with a critical cysteine residue in the tyrosine kinase domain (Fry *et al*., 1998), blocked NRG-1β-induced phosphorylation of this 185 kDa

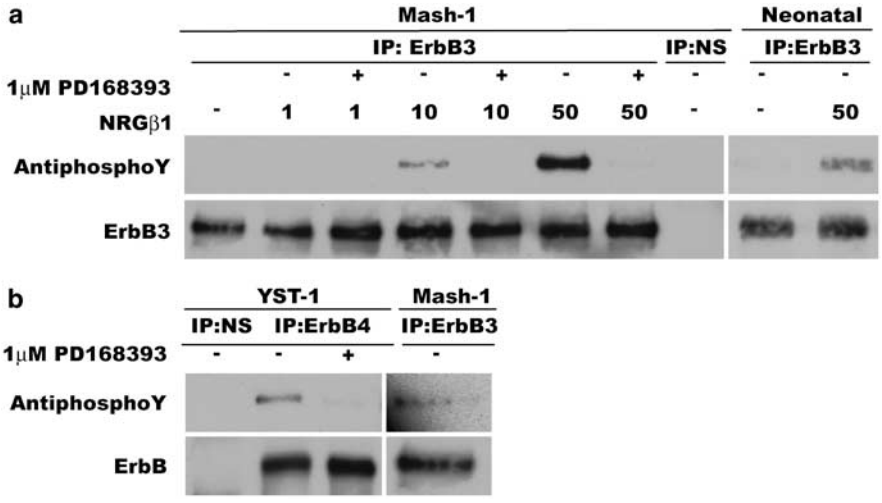

Figure 9 Human MPNST cells are NRG-1 responsive and demonstrate constitutive erbB tyrosine phosphorylation that is abolished by treatment with the pharmacologic inhibitor PD168393. (a) (Left panel), To examine NRG-1 responsiveness, Mash-1 cells were stimulated with vehicle (0) or 1, 10 or 50 nM recombinant NRG-1β in the presence (+) or absence (−) of 1 μM PD168393. ErbB3 was immunoprecipitated from lysates of these cells and the blotted immunoprecipitates probed with an anti-phosphotyrosine antibody (top panel), with phosphorylated erbB3 evident as a 185 kDa band. The bottom panel represents the top panel reprobed with an anti-erbB3 antibody. NS, control immunoprecipitation performed using nonimmune rabbit IgG. An induction of erbB phosphorylation is evident in cells stimulated with 10 or 50 nM NRG-1β. Right panel, control neonatal Schwann cells stimulated with NRG-1β. (**b**) Possible constitutive erbB tyrosine phosphorylation in YST-1 MPNST cells was examined by immunoprecipitating erbB4 from lysates of unstimulated YST-1 cells and probing immunoblotted immunoprecipitates with an anti-phosphotyrosine antibody (top panel). Phosphorylated erbB4 was evident as a 185 kDa species that was abolished by pretreating cells with PD168393. Longer exposures of the unstimulated Mash-1 immunoprecipitates illustrated in panel a likewise show evidence of constitutive erbB3 phosphorylation in this line (right panel). (Bottom panels), Reprobe of the blots shown in the top panels with an anti-erbB4 (left) or anti-erbB3 (right) antibody

protein (Figure 9a), confirming its identification as erbB3.

The coexpression of NRG-1 and its receptors in human MPNST cell lines suggests that autocrine or paracrine NRG-1 signaling may promote constitutive activation of erbB receptors expressed by neoplastic Schwann cells in MPNSTs. To test this hypothesis, we immunoprecipitated erbB4 from unstimulated YST-1 cells (a line that expresses erbB3 and erbB4 in the absence of detectable EGFR) and probed the blotted immunoprecipitates with an anti-phosphotyrosine antibody. A phosphorylated protein of the expected 185 kDa mass was readily detectable in unstimulated YST-1 cells (Figure 9b, left panel). The presence of this phosphorylated species was abolished by pretreating YST-1 cells with PD168393 (Figure 9b, left panel). Longer exposures of the blots shown in Figure 9a likewise demonstrated the presence of a lower level of phosphorylated erbB3 in unstimulated Mash-1 cells (Figure 9b, right panel). We conclude that erbB receptors expressed in Mash-1 and YST-1 cells are constitutively phosphorylated.

To test the hypothesis that human MPNST mitogenesis is dependent on constitutive activation of the NRG-1/erbB signaling pathway, we challenged Mash-1, NMS-2, NMS-2PC and YST-1 cells with 1, 10, 100 or 1000 nM PD168393. After 24 h of inhibition, [^{3}H]thymidine incorporation in cells receiving vehicle was compared to that in cells treated with PD168393. We found that treatment with PD168393 reduced DNA synthesis in all four MPNST cell lines in a concentration-dependent manner (Figure 10), although some cell lines were more sensitive to this treatment than others (e.g., compare Mash-1 and YST-1 cells). We also examined the effects that treatment with 1, 10 or 20 μM concentrations of PD158780, a 4-[ar(alk)ylamino]pyridopyrimidine derivative that specifically inhibits erbB receptors by competing with ATP for binding to the erbB tyrosine kinase domain (Fry *et al*., 1997), had on DNA synthesis in these human MPNST cell lines. Consistent with our previous demonstration that PD158780 effectively reduces erbB tyrosine phosphorylation and DNA synthesis in JS1 cells (Frohnert *et al*., 2003a) (a line derived from a chemically induced rodent MPNST), we found that this mechanistically distinct erbB inhibitor also markedly reduced DNA synthesis in all four human MPNST cell lines (data not shown).

Discussion

We have previously shown that constitutive activation of the NRG-1/erbB signaling pathway is essential for the proliferation of an MPNST cell line derived from an EtNU-induced rodent tumor (Frohnert *et al*., 2003a) and that NRG-1 overexpression in the Schwann cells of transgenic mice induces the formation of MPNST-like neoplasms (Huijbregts *et al*., 2003). The results presented here demonstrate that human neurofibromas and

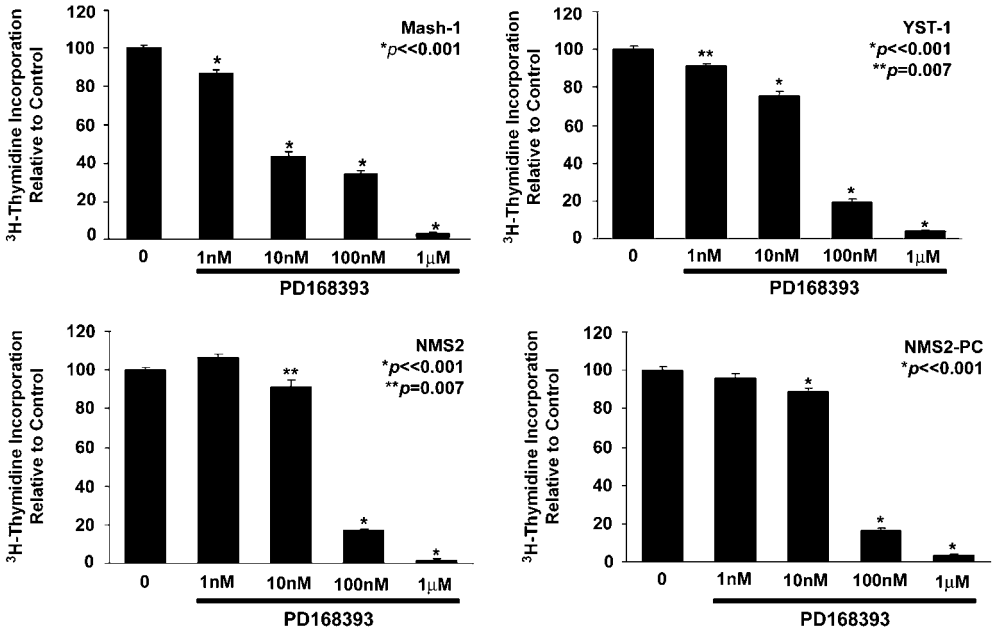

Figure 10 The erbB inhibitor PD168393 inhibits DNA synthesis in human MPNST cells in a concentration-dependent fashion. Bars indicate [^{3}H]thymidine incorporation relative to controls (untreated cells) in Mash-1, YST-1, NMS2 and NMS2-PC cells (indicated above each graph). Standard errors of the mean are indicated for each condition. *P*-values for the indicated treatment conditions are for comparisons to control. Experiments were performed in triplicate, with 6–8 replicates per condition performed in each experiment

MPNSTs likewise express multiple NRG-1 isoforms in combination with the erbB membrane tyrosine kinases mediating NRG-1 responses. We have also found that four human MPNST cell lines similarly coexpress multiple NRG-1 isoforms and erbB kinases, that erbB receptors expressed by these cells are constitutively phosphorylated and that two structurally and mechanistically distinct pharmacologic inhibitors of erbB kinases reduce erbB phosphorylation in these cells and inhibit their proliferation. Considered together, these observations support the hypothesis that inappropriate activation of the NRG-1/erbB signaling pathway promotes neoplastic Schwann cell proliferation in human MPNSTs. Our results also raise some intriguing new questions regarding the role specific NRG-1 isoforms and erbB receptors play in human peripheral nerve sheath tumorigenesis and the possible significance of their coexpression with the EGFR.

Three lines of evidence indicate that NRG-1 is locally synthesized by Schwann cells within neurofibromas and MPNSTs. First, using an antibody recognizing the EGF-like common domain present within all functional NRG-1 isoforms, we identified multiple NRG-1-like immunoreactive proteins in all of the neurofibromas and MPNSTs we examined. Since NRG-1 mRNAs are also present within neurofibromas and MPNSTs, it is likely that much of the NRG-1 detected within each tumor was locally synthesized rather than representing NRG-1 protein derived from the circulation. This hypothesis is further substantiated by our finding that a second antibody recognizing the carboxy terminus of NRG-1 isoforms with an 'a' variant carboxy terminus also labels a subset of the NRG-1 proteins detected by the pan NRG-1 antibody in neurofibromas and MPNSTs; the 'a' variant carboxy-terminal domain is intracellular and is not thought to be released from cells synthesizing NRG-1 transmembrane precursors (Bao *et al*., 2003). Finally, we have demonstrated that multiple NRG-1 proteins and mRNAs are expressed by four permanent cell lines derived from human MPNSTs. Taken together, these findings support the hypothesis that neoplastic Schwann cells themselves produce NRG-1, which then acts in an autocrine and/or paracrine manner to promote neoplastic Schwann cell proliferation.

The structure of the NRG-1 isoforms predicted by neurofibroma- and MPNST-derived NRG-1 cDNAs also has important implications for the potential signaling capabilities of these proteins. We have found that mRNAs encoding NRG-1 transmembrane precursors predominate in peripheral nerve sheath tumors, with transcripts encoding directly secreted NRG-1 isoforms being undetectable in these neoplasms. NRG-1 transmembrane precursors are thought to act when they are proteolytically cleaved, releasing the NRG-1-extracellular domain containing the receptor-binding EGF-like domain. The released extracellular domain then binds to and activates erbB receptors expressed on the same or neighboring cells. It has recently been found that this proteolytic cleavage also releases the intracellular domain of NRG-1 transmembrane precursors from the surface membrane, allowing it to be translocated into the nucleus of the NRG-1-expressing cell, where this domain is thought to mediate poorly understood 'backsignaling' events (Bao *et al*., 2003). Although our demonstration that erbB signaling is required for

the proliferation of MPNST cells argues that 'forward' signaling by the NRG-1 extracellular domain is essential for peripheral nerve sheath tumorigenesis, the preferential expression of NRG-1 transmembrane precursors in peripheral nerve sheath tumors raises the question of whether backsignaling by the NRG-1 intracellular domain also makes an important contribution to this process. As NRG-1 signaling in peripheral nerve sheath tumors is potentially dependent on proteolytic cleavage of transmembrane precursors, inhibitors of the enzymes that cleave NRG-1 transmembrane isoforms (e.g., matrix metalloproteases; Montero *et al*., 2000; Wakatsuki *et al*., 2004) may be useful agents for the treatment of neurofibromas and MPNSTs.

In 1986, Brockes *et al*. (1986) reported that a heparin-binding GGF-like activity was present in a single MPNST and that two of the five neurofibromas they studied contained intermediate to high levels of a similar activity. We have found that mRNAs encoding class II (GGF) NRG-1 isoforms are expressed in human neurofibromas and MPNSTs. We did not detect mRNA encoding NRG-2, a related factor with similar biochemical properties, in any of these tumors using RT–PCR (data not shown). Considered together, these findings suggest that the GGF-like proteins detected by Brockes *et al*. were class II (GGF) NRG-1 isoforms, a group of molecules that act as secreted factors and accumulate at high concentrations in structures such as Schwann cell basement membranes. We also found that the NRG-1 isoforms expressed by neurofibromas and MPNSTs include class III (SMDF/CRD-NRG) NRG-1 variants. Unlike GGF isoforms, class III NRG-1 proteins remain membrane-associated (Falls, 2003) and thus, likely function solely as juxtacrine signaling molecules. The differing phenotypes of transgenic mice overexpressing class II (Huijbregts *et al*., 2003) and class III (Michailov *et al*., 2004) NRG-1 isoforms in the peripheral nervous system also indicate that members of these NRG-1 subfamilies have distinct effects on the phenotype of Schwann cells. Given these functional differences, it will be of great interest to establish what role class II and III NRG-1 isoforms play in the pathogenesis of peripheral nerve sheath tumors.

Our findings demonstrate that cells within neurofibromas and MPNSTs express combinations of erbB receptors that render them potentially NRG-1 responsive. As the human MPNST cell lines we have studied also express these receptors, it seems likely that a major portion of the erbB protein expressed in neurofibromas and MPNSTs is associated with neoplastic Schwann cells. These observations, considered together with our findings that NRG-1 is expressed in neurofibromas and MPNSTs, that the erbB receptors expressed in human MPNST cell lines are constitutively phosphorylated and that two mechanistically distinct ErbB kinase inhibitors inhibit DNA synthesis in these lines, support the hypothesis that neoplastic Schwann cell proliferation is driven by autocrine and/or juxtacrine signaling in these peripheral nerve sheath tumors. Interestingly, however, the particular combination of erbB kinases expressed in an individual tumor is variable. Since erbB2, erbB3 and erbB4 differ in their ability to activate specific cytoplasmic signaling pathways (Yarden and Sliwkowski, 2001), it is likely that NRG-1 signaling will have overlapping, but distinct, effects on the phenotype of neoplastic Schwann cells expressing different profiles of erbB receptors. Consistent with previous observations in human neoplasms and transgenic mouse models (DeClue *et al*., 2000; Li *et al*., 2002), we have also found that EGFR is present in many human neurofibromas and MPNSTs, commonly being coexpressed with NRG-1 receptors. Although the EGFR does not bind NRG-1, it is capable of interacting with other activated erbB receptors, allowing the EGF and NRG-1 receptor systems to 'crosstalk' and modify the cellular responses evoked by EGFR and NRG-1 receptor ligands (Yarden and Sliwkowski, 2001). These findings thus suggest that effects mediated through the erbB kinases expressed by human neurofibromas and MPNSTs may be variable, with the phenotype of neoplastic Schwann cells being determined, in part, by the combination of erbB receptors expressed by individual cells.

In summary, our findings support the hypothesis that constitutive activation of the NRG-1/erbB signaling pathway promotes the proliferation of neoplastic Schwann cells in human neurofibromas and MPNSTs. The effectiveness erbB neutralizing antibodies (e.g., trastuzumab (Herceptin)) and small molecular erbB inhibitors (e.g., PD168393 and PD158780) have shown in preclinical and/or clinical studies with other tumor types raises the intriguing question of whether agents such as these may be effective in treating human neurofibromas and MPNSTs. Determining the role specific NRG-1 isoforms and erbB kinases play in the pathogenesis of human peripheral nerve sheath tumors will also be essential for developing new, more effective treatments for these therapeutically challenging Schwann cell neoplasms.

Materials and methods

Study cases

Protocols for studies with human tissue were approved by the University of Alabama at Birmingham Institutional Review Board for Human Use. Frozen neurofibroma and MPNST tissue was provided by the Southern Division of the Cooperative Human Tissue Network/University of Alabama at Birmingham Tumor Bank (Director: William Grizzle, MD, PhD). Paraffin-embedded blocks of neurofibroma and MPNST tissue were obtained from the files of the Department of Pathology of the University of Alabama School of Medicine (Birmingham, AL, USA). Patient ages, sex, race, NF1 status, and tumor location for the fresh and paraffin-embedded tissues used in our studies are provided in Tables 1 and 2, respectively.

Antisera and immunohistochemical reagents

We have previously described the production and characterization of a rabbit polyclonal antibody that specifically recognizes the EGF-like common domain found in all biologically active NRG-1 isoforms (a 'pan'-NRG antibody)

(Carroll *et al*., 1997). A mouse monoclonal antibody recognizing an epitope in the EGFR (residues 996–1002) was obtained from MP Biomedicals (clone c11; Irvine, CA, USA). A mouse monoclonal antibody directed toward the C-terminus of human erbB2 (residues 1242–1255) was purchased from Oncogene Research Products (Ab-3; La Jolla, CA, USA). The mouse IgM monoclonal antibody RTJ.1 recognizes the C-terminal domain of erbB3; this antibody and an isotype-matched negative control clone (C48-6) were obtained from BD Biosciences PharMingen (San Diego, CA, USA). Affinity-purified rabbit polyclonal antisera for EGFR (sc-03), ErbB3 (sc-285), erbB4 (sc-283) and the NRG-1 'a'-carboxy-terminal domain (sc-348) were obtained from Santa Cruz Biotechnology (Santa Cruz, Ca, USA). Rabbit polyclonal antibodies recognizing S100β (#Z0311) and GFAP (#Z0334) and an anti-desmin mouse monoclonal antibody (clone D33) were purchased from Dako (Carpinteria, CA, USA). The mouse anti-collagen type IV monoclonal antibody (clone PHM-12) used in our studies was from Ventana Medical Systems (Tucson, AZ, USA). A mouse monoclonal antibody recognizing smooth muscle actin (clone 1A4) was purchased from NeoMarkers (Fremont, CA, USA). A rabbit anti-NSE antibody was obtained from Chemicon International (Temecula, CA, USA). The mouse monoclonal antibody recognizing GAPDH (clone 6C5) was purchased from Advanced ImmunoChemical Inc. (Long Beach, CA, USA). Nonimmune mouse and rabbit IgGs were obtained from Pierce (Rockford, IL, USA). Horseradish peroxidase (HRP)-conjugated donkey anti-rabbit secondary antibody was from Jackson Immunoresearch Inc. (West Grove, PA, USA). Tyramide signal amplification reagents, including streptavidin-HRP, biotinyl tyramide, amplification diluent, and blocking reagent were purchased from Perkin-Elmer Life and Analytical Science Products (Renaissance TSA-Indirect kit, Boston, MA, USA). DAB peroxidase substrate (SK-4100) was obtained from Vector Laboratories (Burlingame, CA, USA).

RT–PCR analyses of NRG-1 isoforms expressed in peripheral nerve sheath tumors and MPNST cell lines

Our designation of NRG-1 domains follows the nomenclature of Peles and Yarden (1993). The common forward oligonucleotide used for amplification of sequences encoding the EGF-like and juxtamembrane domains of NRG-1 corresponds to nucleotides 631–648 of human NDF (also known as class I NRG-1 isoforms; GenBank accession no. U02326) (Wen *et al*., 1994). The reverse oligonucleotide for PCR of NRG-1 transmembrane precursor cDNAs represents nucleotides 811–828 (encoding a portion of the transmembrane domain sequence) of human NDF. This oligonucleotide pair will amplify sequences encoding all possible combinations of EGF-like and juxtamembrane sequences found in NRG-1 transmembrane isoform mRNAs. Secreted NRG-1 isoform cDNAs were amplified using the common forward oligonucleotide in combination with a reverse oligonucleotide corresponding to nucleotides 482–502 of a human NDFβ3 splice variant (GenBank accession no. U02327)(Wen *et al*., 1994). NDF amino-terminal sequences were amplified using oligonucleotides corresponding to nucleotides 484–504 and 887–867 of human NDFβ3 (GenBank accession no. BC006492). GGF (class II NRG-1 isoform) amino-terminal sequences were amplified using oligonucleotides representing nucleotides 429–452 and 900–877 of a human GGFβ3 cDNA (GenBank accession no. L12260). SMDF (class III NRG-1 isoform) NRG-1 amino-terminal sequences were amplified using oligonucleotides corresponding to nucleotides 806–822 and 1231–1210 of a human SMDFβ3 cDNA (GenBank accession no. BC007675).

Single-stranded cDNA for use as a PCR template was synthesized from total cellular RNA isolated from tumor tissue or cultured tumor cells using Trizol reagent (Invitrogen). RNA was reverse transcribed in a 20 μl reaction using random hexamer primers and Moloney murine leukemia virus reverse transcriptase (Superscript Plus, Life Technologies, Gaithersburg, MD, USA). After completion of reactions, samples were diluted to 100 μl with distilled water, boiled for 5 min and stored at -80°C until use.

A 2 μl portion of each cDNA was used as a PCR template in reactions performed for 35 cycles of 94°C for 1 min, 55°C for 1 min and 72°C for 2 min. PCR products were ligated into pCR4-TOPO and ligations transformed into *Escherichi coli* (Top10 strain) as recommended by the manufacturer (Invitrogen Life Technologies, Carlsbad, CA, USA). The sequence of these clones was determined by cycle sequencing using an automated sequencer (ABI Model 373A DNA Sequencing System, Applied Biosystems Inc. Foster City, CA, USA).

Immunohistochemistry for erbB kinases and NRG-1 in tumor sections

Immunohistochemical detection of erbB and NRG-1 proteins was performed on 4- to 5-μm-thick sections of paraffin-embedded tissue using a modified protocol we have previously developed and validated (Gerecke *et al*., 2001). In brief, after deparaffinization of sections in xylenes and graded alcohols, antigen rescue was performed by gently boiling slides in 10 mM citrate buffer (pH 6.0) for 15 min and then allowing them to cool to room temperature for 15 min. Nonspecific binding was blocked by incubating sections for 15 min with TNB blocking buffer (0.1 M Tris-HCl (pH 7.5)/0.15 M NaCl/ 0.5% blocking reagent) at room temperature. Sections were then incubated overnight at 4°C with primary antibodies diluted in blocking buffer (1 : 100 dilution, EGFR clone c11; 1 : 100 dilution, erbB2 Oncogene Ab-3; 1 : 100–1 : 250 dilution, erbB3 monoclonal RTJ.1; 1 : 500 dilution, ErbB4 rabbit polyclonal antibody; 1 : 250–1 : 500 dilution, pan NRG-1 rabbit polyclonal antibody). After three rinses in phosphate-buffered saline (PBS; 10 min per rinse), sections were incubated for 1 h at room temperature with HRP-conjugated secondary antibody (diluted 1 : 250–1 : 500 in blocking buffer). After three washes in PBS, biotinyl tyramide (diluted 1 : 50 in amplification diluent) was applied to tissue sections for 10 min at room temperature. Sections were again washed three times in PBS and then incubated with streptavidin-HRP (diluted 1 : 100 in TNB) for 45 min. After three final washes with PBS, immunoreactive structures were visualized by diaminobenzidine deposition. To confirm the specificity of staining, control slides were treated identically except that primary antibody was replaced with blocking buffer alone. As an additional control, some sections were processed with nonimmune mouse IgG (for EGFR and ErbB2 controls), nonimmune isotype-matched IgM (for erbB3 controls) or nonimmune rabbit IgG (for erbB4 and pan NRG controls) in place of the primary antibodies. No staining was observed in these experiments. For the erbB2, erbB4 and pan NRG-1 antigens, specificity of staining was further confirmed by preincubating antisera with either the immunizing peptide or a nonrelated peptide (10 ng/ml); in all instances, preincubation with the immunizing peptide, but not the nonrelated peptide, abolished the staining pattern observed with primary antibody alone. Following immunostaining, slides were lightly counterstained with hematoxylin, coverslipped and mounted with Permount (Fisher).

Immunoblotting

Lysates for immunoblotting were prepared by homogenizing specimens in Trizol reagent (Invitrogen) according to the manufacturer's protocol. Protein pellets were dissolved in 1% SDS supplemented with protease (Sigma #P8340) and phosphatase (Sigma #P5726) inhibitors diluted 1 : 100–1 : 250. Protein concentrations were determined with a modified Lowry method (*DC* Protein Assay; Bio-Rad, Hercules, CA, USA). Equivalent quantities of protein lysates were resolved on 8% SDS polyacrylamide gels. Membranes were blocked in 5% nonfat dry milk in TBST (0.15 M NaCl, 10 mM Tris (pH 8.0), 0.05% Tween 20) prior to incubation with primary antibody. The following primary antibody concentrations were used for immunoblotting: EGFR (Santa Cruz sc-03; 1 : 1000), erbB-2 (Oncogene Ab-3; 1 : 500–1 : 1000), erbB3 (Santa Cruz sc-285; 1 : 1000), erbB4 (Santa Cruz sc-283; 1 : 1000), pan NRG-1 (1 : 5000) and NRG-1 'a' carboxy terminus (Santa Cruz sc-348; 1 : 1000). HRP-conjugated donkey anti-rabbit and donkey anti-mouse secondary antibodies were used at a 1 : 10000 dilution in 5% milk/TBST. Immunoreactive species were detected by enhanced chemiluminescence (Pierce). In preliminary experiments, we examined the feasibility of using immunoreactivity for GAPDH, β-actin and ERK-2 to verify equivalent loading of neurofibroma and MPNST lysates. However, we found that the highly variable degree of collagenization in neurofibromas and MPNSTs rendered normalization to intracellular housekeeping protein levels problematic. Consequently, equivalent loading and transfer of tumor lysates was verified by Coomassie staining of the PVDF membrane post-transfer, while equivalent loading and transfer of cell line lysates was verified by reprobing blots with an anti-GAPDH antibody. Specificity of immunoblotting was determined for each immunoblot by preincubating the blotting antibody with a 5–10-fold excess of the appropriate immunizing peptide.

MPNST cell lines, neonatal Schwann cells and their culture conditions

The Mash-1 cell line is a human MPNST cell line derived from a skin/chest metastasis in a male NF1 patient (Endo *et al*., 2002) and was obtained from the Cell Bank of the RIKEN BioResource Center (Ibaraki, Japan). The NMS-2 cell line was established from an MPNST arising in the right thigh of a 30-year-old man with NF1 and the NMS-2PC cell line was derived from a retroperitoneal metastasis occurring 9 months later in the same patient (Imaizumi *et al*., 1998). NMS-2 and NMS-2PC cells were generously provided by Dr Akira Ogose (Department of Orthopedic Surgery, Niigata University, Niigata, Japan). The YST-1 cell line was derived from an epithelioid MPNST that occurred in the upper arm of an 8-year-old girl with no clinical evidence of NF1 (Nagashima *et al*., 1990). YST-1 cells were kindly provided by Dr Yoji Nagashima (Department of Pathology, Yokohama City University School of Medicine, Yokohama, Japan). NMS-2, NMS-2PC and YST-1 cell lines were maintained in RPMI medium supplemented with 10% heat-inactivated fetal bovine serum (FBS), 10 IU/ml penicillin and 10 μg/ml streptomycin. Mash-1 cells were maintained in a 1 : 1 mixture of Keratinocyte SFM medium (Invitrogen; supplemented with 5 ng/ml EGF and 50 μg/ml bovine pituitary extract) and DMEM (supplemented with 5% heat-inactivated FBS). Cultures of neonatal Schwann cells were established from the sciatic nerves of postnatal day 0–2 Sprague–Dawley rat pups using our previously described methodology (Frohnert *et al*., 2003a) and maintained in DMEM supplemented with 10% FBS.

Immunostaining and RT–PCR analyses of marker expression in MPNST cell lines

To detect S100β immunoreactivity, MPNST cells were plated at low density in chamber slides and allowed to adhere overnight. The next morning, slides were fixed for 30 min at room temperature with 4% paraformaldehyde and then rinsed three times with PBS (5 min per wash). Nonspecific binding was blocked by incubating cells for 30 min in blocking buffer (PBS containing 1% bovine serum albumin, 0.2% nonfat dry milk and 0.3% Triton X-100). Cells were then incubated overnight at 4°C with anti-S100β antibody diluted 1 : 200 in blocking buffer. The next morning, cells were rinsed three times with PBS and then incubated for 1 h at room temperature with Cy3-conjugated donkey anti-rabbit secondary antibody (Jackson Immunoresearch) diluted 1 : 250 in blocking buffer. Following three more rinses in PBS, slides were mounted using 1 : 1 PBS : glycerol and examined by fluorescence microscopy.

To construct tissue arrays, MPNST cells were grown to confluence and then removed from their substrate nonenzymatically using Cellstripper (Mediatech, Herndon, VA, USA). Cells were pelleted and mixed with an equal volume of HistoGel specimen processing gel (Richard-Allan Scientific, Kalamazoo, MI, USA). After coagulation at 4°C, cell pellets were transferred to cassettes and fixed in 10% formalin. Fixed pellets were then dehydrated through graded alcohols and xylenes and paraffin embedded. Then, 1.5 mm cores were taken in triplicate from donor blocks of MPNST cell pellets and human controls (paraffin blocks of normal adrenal medulla, a breast carcinoma, normal pituitary, normal kidney, SKOV-3 ovarian carcinoma cells, MCF-7 breast carcinoma cells, PC-3 prostate carcinoma cells and DU145 prostate carcinoma cells) and used to construct tissue arrays. Sections (4–5 μm) were prepared, deparaffinized with xylene and rehydrated through graded ethanol to PBS. After blocking nonspecific binding by incubating rehydrated sections for 30 min in blocking buffer, sections were incubated with primary antibody or nonimmune IgG for 2 h at room temperature. Dilutions of primary antibodies were: collagen type IV, 1 : 50; GFAP, 1 : 500; NSE, 1 : 1000; smooth muscle actin, 1 : 1000; and desmin, 1 : 50. Following incubation with primary antibodies, sections were rinsed three times with PBS and then incubated with HRP-conjugated secondary antibodies for 1 h at room temperature. Following three more washes with PBS, immunoreactivity was detected by diaminobenzidine deposition. Sections were lightly counterstained with hematoxylin and mounted with Permount for light microscopic examination.

For RT–PCR analyses, 2 μl of cDNAs synthesized from total cellular RNA as described above was used as a PCR template in reactions performed for 35 cycles of 94°C for 1 min, 55°C for 1 min and 72°C for 2 min. Primers were designed from the reference sequence deposited for each tested marker in Entrez Gene using PrimerSelect software (Version 3.10; DNAStar Inc.).

DNA synthesis assays

To assay DNA synthesis in human MPNST cell lines, 40 000 cells/well were plated in 24-well plates in RPMI medium containing 10% FBS and allowed to attach overnight. The next morning, PD168393 (Calbiochem, La Jolla, CA, USA), PD158780 (Calbiochem) or vehicle (DMSO) was added to each well. At 12 h after addition of vehicle or erbB inhibitors, 1 μCi/ml of [^{3}H]thymidine was added to each well. After 12 h, [^{3}H] thymidine incorporation was assayed using our previously described methodology (Frohnert *et al*., 2003a, b).

All experiments were performed in triplicate, with six replicates/condition performed in each experiment. One-way ANOVA, followed by a Tukey *post hoc* test, was performed on the resulting data, with $P<0.05$ considered statistically significant.

Acknowledgements
We thank Dr Kevin A Roth (Department of Pathology, UAB) for helpful comments on this manuscript. This work was supported by National Institute of Neurological Disorders and Stroke Grant R01 NS048353.

References

Bao J, Wolpowitz D, Role LW and Talmage DA. (2003). *J. Cell Biol.*, **161,** 1133–1141.
Bargmann CI, Hung MC and Weinberg RA. (1986). *Cell*, **45,** 649–657.
Bargmann CI and Weinberg RA. (1988). *EMBO J.*, **7,** 2043–2052.
Ben-Baruch N and Yarden Y. (1994). *Proc. Soc. Exp. Biol. Med.*, **206,** 221–227.
Birindelli S, Perrone F, Oggionni M, Lavarino C, Pasini B, Vergani B, Ranzani GN, Pierotti MA and Pilotti S. (2001). *Lab. Invest.*, **81,** 833–844.
Brockes JP, Breakefield XO and Martuza RL. (1986). *Ann. Neurol.*, **20,** 317–322.
Carpenter G. (2003). *Exp. Cell Res.*, **284,** 66–77.
Carroll SL, Miller ML, Frohnert PW, Kim SS and Corbett JA. (1997). *J. Neurosci.*, **17,** 1642–1659.
Carroll SL and Stonecypher MS. (2004). *J. Neuropathol. Exp. Neurol.*, **63,** 1115–1123.
Carroll SL and Stonecypher MS. (2005). *J. Neuropathol. Exp. Neurol.*, **64,** 1–9.
DeClue JE, Heffelfinger S, Benvenuto G, Ling B, Li S, Rui W, Vass WC, Viskochil D and Ratner N. (2000). *J. Clin. Invest.*, **105,** 1233–1241.
Di Marco E, Pierce JH, Knicley CL and Di Fiore PP. (1990). *Mol Cell Biol*, **10,** 3247–3252.
Dong Z, Brennan A, Liu N, Yarden Y, Lefkowitz G, Mirsky R and Jessen KR. (1995). *Neuron*, **15,** 585–596.
Ducatman BS, Scheithauer BW, Piepgras DG, Reiman HM and Ilstrup DM. (1986). *Cancer*, **57,** 2006–2021.
Endo H, Utani A and Shinkai H. (2002). *Br. J. Dermatol.*, **147,** 821–822.
Falls DL. (2003). *Exp. Cell Res.*, **284,** 14–30.
Ferner RE and Gutmann DH. (2002). *Cancer Res.*, **62,** 1573–1577.
Ferner RE and O'Doherty MJ. (2002). *Curr. Opin. Neurol.*, **15,** 679–684.
Frohnert PW, Stonecypher MS and Carroll SL. (2003a). *Glia*, **43,** 104–118.
Frohnert PW, Stonecypher MS and Carroll SL. (2003b). *J. Neuropathol. Exp. Neurol.*, **62,** 520–529.
Fry DW, Bridges AJ, Denny WA, Doherty A, Greis KD, Hicks JL, Hook KE, Keller PR, Leopold WR, Loo JA, McNamara DJ, Nelson JM, Sherwood V, Smaill JB, Trumpp-Kallmeyer S and Dobrusin EM. (1998). *Proc. Natl. Acad. Sci. USA*, **95,** 12022–12027.
Fry DW, Nelson JM, Slintak V, Keller PR, Rewcastle GW, Denny WA, Zhou H and Bridges AJ. (1997). *Biochem. Pharmacol.*, **54,** 877–887.
Gerecke KM, Wyss JM, Karavanova I, Buonanno A and Carroll SL. (2001). *J. Comp. Neurol.*, **433,** 86–100.
Graus-Porta D, Beerli RR, Daly JM and Hynes NE. (1997). *EMBO J.*, **16,** 1647–1655.
Gutmann DH. (2001). *Hum. Mol. Genet.*, **10,** 747–755.
Gutmann DH, Aylsworth A, Carey JC, Korf B, Marks J, Pyeritz RE, Rubenstein A and Viskochil D. (1997). *JAMA*, **278,** 51–57.
Hudziak RM, Schlessinger J and Ullrich A. (1987). *Proc. Natl. Acad. Sci. USA*, **84,** 7159–7163.
Huijbregts RPH, Roth KA, Schmidt RE and Carroll SL. (2003). *J. Neurosci.*, **23,** 7269–7280.
Imaizumi S, Motoyama T, Ogose A, Hotta T and Takahashi HE. (1998). *Virchows Arch.*, **433,** 435–441.
Kluwe L, Friedrich R and Mautner VF. (1999). *Genes Chromosomes Cancer*, **24,** 283–285.
Kourea HP, Cordon-Cardo C, Dudas M, Leung D and Woodruff JM. (1999a). *Am. J. Pathol.*, **155,** 1885–1891.
Kourea HP, Orlow I, Scheithauer BW, Cordon-Cardo C and Woodruff JM. (1999b). *Am. J. Pathol.*, **155,** 1855–1860.
Lakkis MM and Tennekoon GI. (2000). *J. Neurosci. Res.*, **62,** 755–763.
Legius E, Dierick H, Wu R, Hall BK, Marynen P, Cassiman JJ and Glover TW. (1994). *Genes Chromosomes Cancer*, **10,** 250–255.
Legius E, Marchuk DA, Collins FS and Glover TW. (1993). *Nat. Genet.*, **3,** 122–125.
Li H, Velasco-Miguel S, Vass WC, Parada LF and DeClue JE. (2002). *Cancer Res.*, **62,** 4507–4513.
Menon AG, Anderson KM, Riccardi VM, Chung RY, Whaley JM, Yandell DW, Farmer GE, Freiman RN, Lee JK, Li FP, Barker DF, Ledbetter DH, Kleider A, Martuza RL, Gusella JF and Seizinger BR. (1990). *Proc. Natl. Acad. Sci. USA*, **87,** 5435–5439.
Metheny LJ, Cappione AJ and Skuse GR. (1995). *J. Neuropathol. Exp. Neurol.*, **54,** 753–760.
Michailov GV, Sereda MW, Brinkmann BG, Fischer TM, Haug B, Birchmeier C, Role L, Lai C, Schwab MH and Nave KA. (2004). *Science*, **304,** 700–703.
Montero JC, Yuste L, Diaz-Rodriguez E, Esparis-Ogando A and Pandiella A. (2000). *Mol. Cell. Neurosci.*, **16,** 631–648.
Morrissey TK, Levi ADO, Nuijens A, Sliwkowski MX and Bunge RP. (1995). *Proc. Natl. Acad. Sci. USA*, **92,** 1431–1435.
Nagashima Y, Ohaki Y, Tanaka Y, Sumino K, Funabiki T, Okuyama T, Watanabe S, Umeda M and Misugi K. (1990). *Virchows Archiv. B.*, **59,** 321–327.
Nielsen GP, Stemmer-Rachamimov AO, Ino Y, Moller MB, Rosenberg AE and Louis DN. (1999). *Am. J. Pathol.*, **155,** 1879–1884.
Nikitin AY, Ballering LAP, Lyons J and Rajewsky MF. (1991). *Proc. Natl. Acad. Sci. USA*, **88,** 9939–9943.
Parada LF. (2000). *Biochim. Biophys. Acta*, **1471,** M13–M19.
Peles E and Yarden Y. (1993). *BioEssays*, **15,** 815–824.
Perry A, Kunz SN, Fuller CE, Banerjee R, Marley EF, Liapis H, Watson MW and Gutmann DH. (2002). *J. Neuropathol. Exp. Neurol.*, **61,** 702–709.
Perry A, Roth KA, Banerjee R, Fuller CE and Gutmann DH. (2001). *Am. J. Pathol.*, **159,** 57–61.
Rahmatullah M, Schroering A, Rothblum K, Stahl RC, Urban B and Carey DJ. (1998). *Mol. Cell. Biol.*, **18,** 6245–6252.
Rutkowski JL, Wu K, Gutmann DH, Boyer PJ and Legius E. (2000). *Hum. Mol. Genet.*, **9,** 1059–1066.
Sherman L, Sleeman JP, Hennigan RF, Herrlich P and Ratner N. (1999). *Oncogene*, **18,** 6692–6699.
Sherman LS, Atit R, Rosenbaum T, Cox AD and Ratner N. (2000). *J. Biol. Chem.*, **275,** 30740–30745.

Tucker T and Friedman JM. (2002). *Clin. Genet.*, **62,** 345–357.
Tzahar E, Waterman H, Chen X, Levkowitz G, Karunagaran D, Lavi S, Ratzkin BJ and Yarden Y. (1996). *Mol. Cell. Biol.*, **16,** 5276–5287.
Vogel KS, Klesse LJ, Velasco-Miguel S, Meyers K, Rushing EJ and Parada LF. (1999). *Science*, **286,** 2176–2179.
Wakatsuki S, Kurisaki T and Sehara-Fujisawa A. (2004). *J. Neurochem.*, **89,** 119–123.
Wallace MR, Rasmussen SA, Lim IT, Bray BA, Zori RT and Muir D. (2000). *Genes Chromosomes Cancer*, **27,** 117–123.
Weiner DB, Liu J, Cohen JA, Williams WV and Greene MI. (1989). *Nature*, **339,** 230–231.
Wen D, Suggs SV, Karunagaran D, Liu N, Cupples RL, Luo Y, Janssen AM, Ben-Baruch N, Trollinger DB, Jacobsen VL, Meng S-Y, Lu HS, Hu S, Chang D, Yang W, Yanigahara D, Koski RA and Yarden Y. (1994). *Mol. Cell. Biol.*, **14,** 1909–1919.
Woodruff JM, Kourea HP, Louis DN and Scheithauer BW. (2000). Pathology and Genetics of Tumours of the Nervous System, First Edition. Kleihues P and Cavenee WK (ed). IARC Press: Lyon, pp. 172–174.
Yarden Y and Sliwkowski M. (2001). *Nat. Rev. Mol. Cell Biol.*, **2,** 127–137.
Zhu Y and Parada LF. (2001). *Exp. Cell Res.*, **264,** 19–28.